# Single-Walled BN Nanostructures

E. Bengu and L. D. Marks

*Northwestern University, Department of Materials Science and Engineering, Evanston, Illinois 60208*
(Received 26 September 2000)

We describe *in situ* synthesis and characterization of single-walled BN nanotubes terminated by fullerenelike structures using electron-cyclotron resonance nitrogen and electron beam boron sources onto polycrystalline tungsten substrates. Detailed comparisons of experimental high-resolution electron microscopy images and simulations based upon molecular models show a dominance of kinks and bends involving fourfold and eightfold ring structures as against fivefold or sevenfold which have been found with carbon. Analysis of the structures as a function of film thickness indicates that they are growing by addition of atoms to the exposed ends of single sheets, not at the substrate-nanostructure interface.

Since the discoveries of $C_{60}$ [1] and carbon nanotubes [2–4], similar structures have been proposed for BN [5]. BN nanotubes are expected to have unique electronic [6,7] and mechanical properties [8,9], for instance, to be semiconducting with a gap of roughly 5.5 eV independent of tube diameter, number of layers, and chirality [10], unlike carbon nanotubes [11,12]. Although synthesis of multiwall BN nanotubes [13], concentric fullerenes [14], and nanoarches [15,16] has been reported, evidence for the presence of single-wall BN structures is limited [17–19]. In general, rectangular terminations have been observed (see [20] and references therein), which were interpreted in terms of closure via fourfold ring structures, although an alternative interpretation via nitrogen-rich pentagons has also been proposed [20]. All these reports have used images obtained after the samples were transferred through air and often after postprocessing steps, so it is never clear that chemisorption or reaction with water vapor or oxygen has not introduced artifacts.

We report here the use of a low-energy electron-cyclotron resonance (ECR) plasma to deposit single-layer BN nanostructures and detailed, *in situ* high-resolution electron microscopy (HREM) of them. By comparison with simulated images, we show that single-wall nanostructures contain both fourfold and eightfold rings. In addition, we show that the growth is at the exposed open ends of the nanostructures, not at the metal-nanostructure interface.

Electrotransparent substrates of polycrystalline tungsten were prepared by jet polishing in a sodium hydroxide-water solution, then introduced into the SPEAR system [21,22]. The substrates were cleaned by repeated cycles of sputtering and annealing until well ordered and clean. The presence of impurities on the surfaces was examined by x-ray photoelectron spectroscopy (XPS). The single-layer nanostructures were deposited on these substrates at temperatures between 300–800 °C and a pressure of around $10^{-3}$ Pa in a UHV baked system with a $10^{-8}$ Pa base pressure using a negative substrate bias of 300–600 V dc. Typical deposition rates were of the order of 0.5–3 Å per second. For boron, a conventional electron-beam evapora-

tion source was used, while nitrogen ions were provided via an Astex Compact ECR source. Deposited films were transferred *in situ* to a UHV surface analysis system with $2 \times 10^{-9}$ Pa base pressure [21,22] where chemical analysis was performed using XPS. The acquired spectra were then compared to previously measured reference spectra from bulk *h*-BN and *c*-BN which indicated a stoichiometry with a B:N ratio of $1 \pm 0.1$. These samples were then transferred under UHV conditions to a 300 kV transmission electron microscope [21,22], and analyzed at a pressure of $2.6 \times 10^{-9}$ Pa. Since the samples were never exposed to air, we can exclude artifacts due to chemisorption.

The character of the films depended weakly on the ion flux, substrate bias, and substrate temperature. BN films deposited at high temperatures (600 °C) and bias settings ($-400$ V) displayed a structure similar to a woolen yarn with single-wall BN structures covering the substrate surface, most clearly visible projecting out into vacuum at the profile edge of the sample. All the evidence indicated that the growth observed at the profile edge was the same as that above the substrate, but for the latter the visibility of the nanostructures was not as clear. These features ranged from relatively smooth conical features, as shown in Fig. 1, to single-wall nanotubes and BN fullerenes (see Fig. 2). A large variation in the dimensions of these as single-wall nanotubes (SWNT) was observed—diameters ranging from 0.5 to 3 nm—in many cases with large changes in diameter over a relatively short distance.

Focusing on the capping of the BN SWNTs, images of several typical configurations are shown in Figs. 3(a), 3(b), and 3(c). An important feature is the presence of particular angles, [arrows 1 and 2 in Fig. 3(a)], an acute angle ranging from 75° to 90°, and an obtuse angle ranging from 125° to 135°, which dominate the observed curvatures. To explain these results, atomic models were constructed using a molecular modeling software package [23]. Our aim was to reproduce the angles and general configuration rather than a precise and quantitative fit which, considering the number of atoms involved, would be close to impossible to
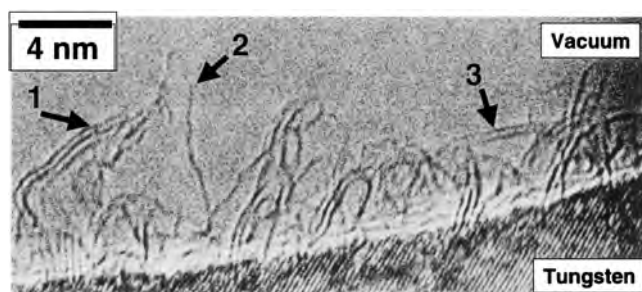
FIG. 1. A high-resolution electron micrograph of single-walled BN nanostructures on tungsten substrate synthesized using ion-beam assisted deposition. Arrows 1 and 3 mark single-walled BN nanotubes (diameter approximately 0.5 nm), and arrow 2 marks a conical feature similar to a nanohorn or nanomountain. The lattice fringes in the substrate are from the (100) planes of tungsten (d spacing 0.223 nm).

achieve. The geometry of these structures was optimized through molecular mechanics, since the average number of atoms in these models (∼400) is rather large for more accurate methods, e.g., *ab initio* quantum mechanics. (Comparison with more accurate quantum mechanical calculations [24] on simpler structures indicates that these will lead to small errors in the atomic positions, too small to have any significant effect on the simulated images.) The relaxed atomic structures shown in Figs. 3(g)–3(i) were then used to simulate HREM images via a multislice algorithm for comparison to the observed images. While raw calculated images showed details within the nanostructures due to the hexagonal arrangement of atoms, after inclusion of statistical noise only the external profile was visible over a very large range of defoci in agreement with the experimental images.

Atomic models with five-, six-, and seven-membered rings (standard for C nanostructures) did not show the
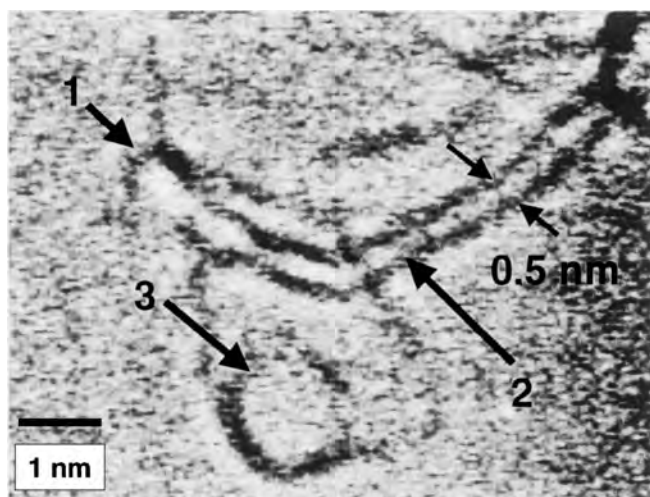


FIG. 2. Images of a capped 0.5 nm nanotube (arrows 1 and 2, respectively) and a BN fullerene roughly 1.35 nm in diameter (arrow 3). The fullerene has a rectangle shape. The diameter of the tubule matches that of a (6,0) tube.

angles experimentally observed and were therefore ruled out. Note that closed surfaces of BN constructed with five-membered rings (also any odd-numbered rings) would contain B-B or N-N bonds, which are thought to be energetically unfavorable [25] (see [20] for an alternative view). Only structures containing four-, six-, and eight-membered rings [Figs. 3(g), 3(h), and 3(i)] produced images [Figs. 3(d), 3(e), and 3(f)] with curvatures comparable to those observed, in particular, the acute and obtuse angles observed experimentally: four-member rings matched the acute angles and eight-membered rings the obtuse ones.

More details about more specific variations in the growth as a function of temperature and substrate bias will be presented elsewhere [24], which include the formation of onions and other structures. We will discuss here one question, namely, the growth mechanism. Similar structures were always observed at the surface of the film essentially independent of the total thickness, indicating that growth is taking place at the ends of open-sheet or nanotube structures and not at the interface with the substrate. Since atoms adsorbed on top of single sheets or nanotubes will be weakly bonded to the
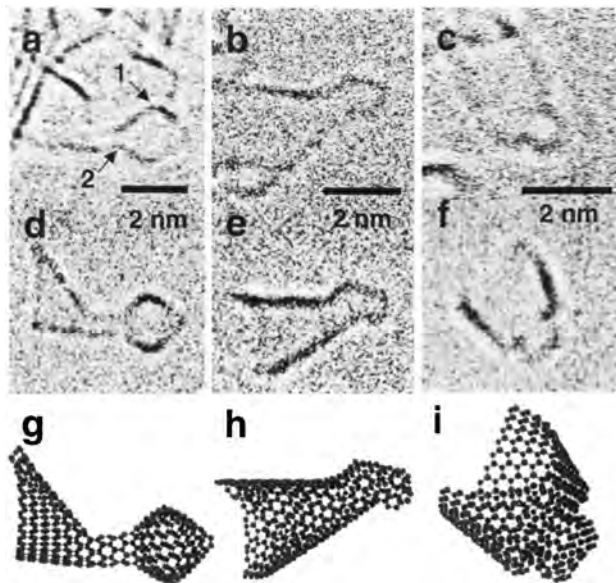


FIG. 3. (a), (b), and (c) Single-walled BN structures observed on tungsten substrates. In (a), we modeled the structure using a $B_{108}N_{108}$ fullerene connected to a large diameter nanotube through a bridging thinner nanotube [as shown in (g)]. The bridging thin section is modeled by a (6,0) nanotube. Arrows 1 and 2 point to the common angles—acute and obtuse, respectively—discussed in the text, modeled using four- and eight-membered BN rings. In (b), a single-walled BN cone [as shown in (h)] that resembles a nanomountain. For (c), an abruptly terminated nanotube with an incomplete fullerene [as shown in (i)]. Shown in (d), (e), and (f) are simulated images to which representative statistical noise has been added, using the relaxed models given in (g), (h), and (i), respectively. Note that only the external shape is clearly visible in the images, not the internal lattice fringes.

sheet (primarily van der Waals with possibly some ionic component, similar to but not the same as graphite), they can rapidly diffuse until they find an open site, similar to stepflow growth at surfaces. Once successful closure is achieved, nucleation of secondary layers around single-wall nanocones, mountains, and/or horns can take place. Conditions favoring the higher mobility of the adatoms (higher temperature) will tend to promote multiwall formation rather than single-wall structures, an effect we have observed [24].

We have described here a new route that takes advantage of low-energy ionic species generated by an ECR plasma source for the stabilization of single-walled BN nanostructures. This method differs from the techniques used in carbon fullerene and nanotube production, such as arc discharge and laser ablation techniques using catalytic metal particles. Rather than gas-phase nucleation of single-walled BN nanostructures, we have achieved direct growth onto a surface enabling us to control the nanostructure evolution using standard parameters which affect nucleation and growth rates. Our method may therefore be exploitable to produce a range of different nanotube coatings of well-controlled structure. This also implies that similar methodologies with direct deposition could be used to produce nanostructured-carbon coatings, as well as other materials such as nanostructured $CN_x$ compounds which could have useful properties for technological applications.

As a final point, we note that the growth conditions herein are similar to those used for cubic BN, where textured growth of the hexagonal BN is observed in the initial stages, e.g., [16] and references therein. We speculate that the single-walled BN structures presented here are another member of the family of fulleritic structures, such as onionlike features and nanoarches formed under intense electron beam irradiation observed for both carbon [26,27] and BN [15,16]. As we have suggested previously [15,16], we believe that the partial $sp^3$ character of the sites at the curved regions of these nanostructures is responsible for nucleation of the cubic phase.

[1] H. W. Kroto, J. R. Heath, S. C. O'Brien, R. F. Curl, and R. E. Smalley, Nature (London) **318**, 162 (1985).
[2] S. Iijima, Nature (London) **354**, 56 (1991).
[3] S. Iijima and T. Ichihashi, Nature (London) **363**, 603 (1993).
[4] D. S. Bethune *et al.,* Nature (London) **363**, 605 (1993).
[5] A. Rubio, J. L. Corkill, and M. L. Cohen, Phys. Rev. B **49**, 5081 (1994).
[6] S. N. Song, X. K. Wang, R. P. H. Chang, and J. B. Ketterson, Phys. Rev. Lett. **72**, 679 (1994).
[7] B. I. Yakobson and R. E. Smalley, Am. Sci. **85**, 324 (1997).
[8] J. Depres, E. Daguerre, and K. Lafdi, Carbon **33**, 87 (1995).
[9] S. Iijima, C. J. Brabec, A. Maiti, and J. Bernholc, J. Chem. Phys. **104**, 2089 (1996).
[10] X. Blase, A. Rubio, S. G. Louie, and M. L. Cohen, Europhys. Lett. **28**, 335 (1994).
[11] R. Saito, M. Fujita, G. Dresselhaus, and M. S. Dresselhaus, Phys. Rev. B **46**, 1804 (1992).
[12] N. Hamada, S. I. Sawada, and A. Oshiyama, Phys. Rev. Lett. **68**, 1579 (1992).
[13] N. G. Chopra *et al.,* Science **269**, 966 (1995).
[14] F. Banhart, M. Zwanger, and H.-J. Muhr, Chem. Phys. Lett. **231**, 98 (1994).
[15] C. Davila-Collazo, E. Bengu, C. Leslie, and L. D. Marks, Appl. Phys. Lett. **72**, 314 (1998).
[16] C. Collazo-Davila, E. Bengu, L. D. Marks, and M. Kirk, Diam. Relat. Mater. **88**, 1091 (1999).
[17] A. Loiseau, F. Willaime, N. Demoncy, G. Hug, and H. Pascard, Phys. Rev. Lett. **76**, 4737 (1996).
[18] D. P. Yu *et al.,* Appl. Phys. Lett. **72**, 1966 (1998).
[19] D. Golberg, Y. Bando, W. Han, K. Kurashima, and T. Sato, Chem. Phys. Lett. **308**, 337 (1999).
[20] P. W. Fowler, K. M. Rogers, G. Seifert, M. Terrones, and H. Terrones, Chem. Phys. Lett. **299**, 359 (1999).
[21] E. Bengu *et al.,* Microsc. Res. Tech. **4**, 295 (1998).
[22] C. Collazo-Davila *et al.,* J. Microsc. Soc. Am. **1**, 267 (1995).
[23] HyperCube, Inc., Gainesville, Florida, HyperChem 5.11, standard version.
[24] E. Bengu, Ph.D. thesis, Northwestern University, 2000; E. Bengu and L. D. Marks (to be published).
[25] F. Jensen and H. Toflund, Chem. Phys. Lett. **201**, 89 (1993).
[26] F. Banhart and P. M. Ajayan, Nature (London) **382**, 433 (1996).
[27] D. Ugarte, Nature (London) **359**, 707 (1992).